Available online at www.sciencedirect.com
SCIENCE DIRECT®
Journal of Solid State Chemistry 177 (2004) 1471–1479
JOURNAL OF SOLID STATE CHEMISTRY
http://elsevier.com/locate/jssc

Elaboration and characterization of $La_2NiO_{4+\delta}$ powders and thin films via a modified sol–gel process

Marie-Laure Fontaine,* Christel Laberty-Robert, Florence Ansart, and Philippe Tailhades

CIRIMAT/LCMIE/UPS-UMR 5085, Université Paul Sabatier, Bât II R1, 118, route de Narbonne, 31062 Toulouse Cedex 04, France

Received 21 May 2003; received in revised form 3 November 2003; accepted 30 November 2003

Abstract

Polycrystalline thin films of $La_2NiO_{4+\delta}$ have been synthesized on yttria stabilized zirconia (YSZ) substrates by dip-coating using a polymeric sol. Crack-free films were obtained after sintering in air at temperatures ranging from 800°C to 1000°C. The microstructure, characterized by SEM, shows the formation of dense polycrystalline films with smooth surface and mean grains size of 140 nm, for films sintered at 1000°C. A correlation between grains size and non-stoichiometry in powders have been made in our processes. The thickness, evaluated for rugosimetry measurements, is thin (80 nm) and is a function of the viscosity of the sol. The higher the thickness, the higher the viscosity. As the non-stoichiometry level is controlled by the oxygen partial pressure, an evolution of non-stoichiometry in thin film has proposed. Then, it is possible by modifying synthesis and processing parameters to prepare thin films with a controlled microstructure (thickness, porosity and non-stoichiometry).

Keywords: Ruddlesden–Popper; Oxides; Sol–gel synthesis; Films; Structure; Morphology; Non-stoichiometry

1. Introduction

The development of solid oxide fuel cells (SOFCs) operating at reduced temperatures (600°C to 800°C) has recently received much attention [1]. The operation of SOFCs at a reduced temperature provides several important advantages including a wider choice of cells and ancillary materials such as use of non-ceramic electrodes and interconnectors. It also allows longer cells life due to decreased interdiffusion between cell components and a lower electrode sintering. Finally, it increases SOFC reliability because of a reduced thermal stress and it reduces cost due to the use of lower cost materials.

Manganite-based SOFCs currently use supported or self-supported $LaSrMnO_{3-\delta}$ (LSM) cathodes with a typical thickness from 50 to 300 μm. This requires SOFCs to operate at about 1000°C to limit cell internal resistances. Thus, one approach to achieve an efficient operation at reduced temperatures is to control the microstructure of the cathode in order to minimize the ohmic losses by increasing the line of the triple boundary point [2,3]. This approach requires a suitable process for the elaboration of thin films. Some recent studies have shown that the elaboration of thin layers of LSM with a porosity around 30% via a polymeric method is made possible by modifying the processing parameters [4].

Another approach is to improve the properties of the perovskite type materials based on lanthanum manganites to increase the density of triple phase boundary. This requires materials exhibiting both good electrical and ionic conductivities. Among the different oxides structures, the Ruddlesden–Popper materials present the most interesting properties because the oxygen ionic diffusion (O^- : the diffusing species along the *c*-axis and O^{2-} : the mobile carriers in the basal (*a*,*b*) plane) in this oxide is some orders of magnitude higher than in perovskite [5,6]. Indeed, this structure can incorporate additional oxygen on the interstitial sites which induces ionic and electronic conductivities [7,8]. This incorporation is often correlated to the preparation technique (temperature, atmosphere, etc.).

Thus, this paper presents the development of a reduced-temperature SOFC cathode based on thin films of new materials such as $La_2NiO_{4+\delta}$ elaborated via a polymeric method. A simple and cost-effective process based on the dip-coating method using a polymeric sol is

*Corresponding author. Fax: +33-056-155-6109.
E-mail address: fontaine@chimie.ups-tlse.fr (M.-L. Fontaine).

0022-4596/$ - see front matter © 2004 Elsevier Inc. All rights reserved.
doi:10.1016/j.jssc.2003.11.032

developed for the elaboration of $La_2NiO_{4+\delta}$ cathodes. The effects of several processing parameters such as viscosity, salt concentration and heating temperature on the structure and microstructure of both powders and thin films are also studied.

2. Experimental procedure

2.1. Sample preparation

The polymeric precursors for synthesizing $La_2NiO_{4+\delta}$ powders and depositing $La_2NiO_{4+\delta}$ thin films are prepared using solutions similar to the one outlined by Pechini [9]. The control of the ratio of the organic compounds to transition metal and the viscosity of the sol before coating are critical to obtain dense and crack-free films. Indeed, when the organic content in the sol is too high, a very large amount of shrinkages appears in the film during calcination, inducing film cracking. Similarly, when the sol viscosity is too high, very thick organic film is obtained and again cracking appears during calcination of the polymeric film. Different sets of experiments are conduced to reduce the overall organic content in the sol while keeping an appropriate number of chelation sites. Sols with different viscosities and ionic concentrations are then prepared.

Reagent grade $La(NO_3)_3 \cdot 6H_2O$ and $Ni(NO_3)_2 \cdot 6H_2O$ nitrates were used as starting salts. These nitrates were dissolved in deionised water in stoichiometric amounts. Since the cation concentration in the sol influences the thickness of the final film, different molar concentrations were investigated. Hexamethylenetetramine (HMTA) resins were added to the mixture as organic carrier. This resin was made from different chelating and polymeric agents such as hexamethylenetetramine, acetic acid and acetylacetone. To study the effect of the nature of the organic precursor on the phase formation, another resin was used. This resin was made from citric acid as chelating agent and ethylene glycol as polymeric one. This resin is referred as P2 resin. The ratio of chelating agent to cation source in the sol (R) was ranging from 2 to 3. The resulting sols were homogenous and precipitate free. They were heated and stirred until the solution reached viscosities ranging from 25 to 60 cP.

To produce powders, the sols were then dehydrated and calcined at 400°C in air during 4 h. Then, the obtained precursors were ground and calcined at a heating rate of 100°C/h, under air during 2 h for temperatures ranging from 800°C to 1000°C.

The precursors solutions were dip-coated onto YSZ substrates. Prior to coatings, the substrates were polished up to a roughness of 10 nm, cleaned by immersion in de-ionized water and drying in air. The precursor-coated films were heated in air at temperatures ranging from 650°C to 1000°C.

2.2. Viscosity

The sol viscosity is measured with a rotating-spindle viscometer (Lamy Tve-05). Sets of measurements are taken at all rotational speeds.

2.3. Thermal analysis

The non-stoichiometry δ of the oxides was determined through Temperature Programmed Reduction (TPR) followed by thermogravimetric analysis. The experiments were carried out in a vertical lug flow reactor. The mass variation of the oxide (initially 80 mg) was followed with a Cahn D200 electrobalance. The sample was first depressed (1 Pa) at room temperature for 1 h and the reactor was then filled with a mixture of H_2/Ar, maintaining a flow of $15\,cm^3\,min^{-1}$. The temperature was then linearly increased with a heating rate of $5\,K\,min^{-1}$ up to 900°C. The technique presents the advantage to quantify selectively the non-stoichiometry oxygen, without preliminary dissolution compared to chemical titration methods. Of course, this method can only be used if the heating of the non-stoichoimetric oxides give rise to the formation of simple stoichiometric oxide such as La_2O_3, and metal as Ni.

Thermogravimetric (TGA) and differential thermal analyses (DTA) were carried out on a Setaram TG-DTA 92 microbalance with 20 mg of sample and alumina as a reference. The experiments were performed in air at a heating rate of $5\,K\,min^{-1}$ from room temperature to 1000°C.

2.4. X-Ray diffraction analysis

The determination of the crystallographic structure of the powders sample was performed by X-ray diffraction with Seifert XRD 3003 TT diffractometer using the Cu$K\alpha$ radiation (α Cu = 0.15418 nm) while the one for thin film was carried out with a Siemens D500 diffractometer using the same radiation.

2.5. Chemical analysis

The chemical compositions were determined by atomic absorption spectroscopy. The La:Ni ratio is found to be slightly higher than 2.

To confirm the non-stoichiometry levels evaluated from thermogravimetric analyses, titrations are done according to a chemical method [6]. The non-stoichiometry level is directly correlated to the content of Ni^{3+} to respect the electroneutrality of the compound. Thus, the determination of Ni^{3+} content via iodometric titration allows the evaluation of δ.

2.6. Electron microscopy

Scanning Electron Microscopy (JEOL- JSM–35CF) was used to determine the morphology and the microstructure resulting from the various sintering conditions.

2.7. Rugosimetry

The thickness of thin film was evaluated with an optical profilometer Zygometer (3D "ZYGO").

3. Results and discussion

3.1. Sol decomposition

The HMTA organic solution is heated at 70°C until it reaches an appropriate viscosity. Then, it is dehydrated at 200°C during a night. The obtained precursor, called "dried gel", is thermogravimetrically characterized to determine the temperature at which the organics fully decompose. Fig. 1 shows the TGA and DTA results for the La_2NiO_4 "dried gel". The thermal analysis of the process turns out to be complex. It reveals a three-step weight loss with corresponding DTA curves. The first weight loss, which occurs at around 90°C, corresponds to the elimination of water that was not removed during the initial solution drying process. The second major weight loss in TGA occurs between 200°C and 500°C, and it is caused by the burnout of pyrolized organics. The third peak, around 700°C, may be attributed to the decomposition of amorphous oxycarbonates formed during the previous steps [10]. There is no more weight loss above 700°C. These results are confirmed by DTA experiments. Indeed, the DTA results show an endothermic reaction starting at 90°C related to water loss and exothermic reactions starting at 300°C related to the pyrolysis of the organic compound. As the weight losses provoked by the decomposition of the organic compounds are high, no weight loss corresponding to the desorption of the excess of oxygen can be observed for temperatures above 700°C. Thus, in order to make sure that all organic compounds are decomposed, the lowest heating temperature for powders and thin films used in this study will be 800°C.

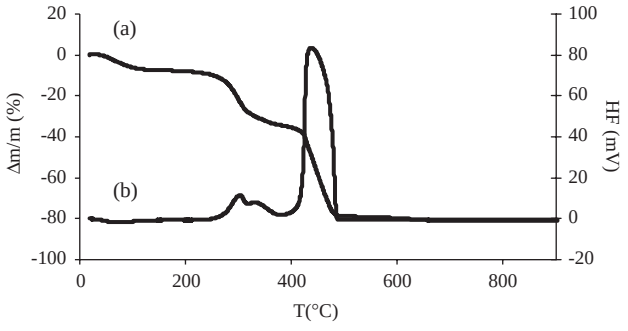

Fig. 1. TGA curve (a) and DTA (b) curve of $La_2NiO_{4+\delta}$ "dried" gel under air.

Studies on $LaSrMnO_3$ films show that the thickness of the film is related to the ionic concentration [10]. Accordingly, the first step is to determine the limit concentration, which will allow us to prepare thick films by keeping the Ruddlesden Popper phase. For this study, different polymeric sols with various ionic concentrations ranging from 0.15 to 0.60 mol L^{-1} are synthesized. Only the concentration of 0.15 mol L^{-1} leads to the formation of the pure phase. For concentrations higher than 0.15 mol L^{-1}, $La_3Ni_2O_7$ and La_2O_3 oxides appear. Thus, the limit concentration allowing the synthesis of thick films with the Ruddlesden Popper phase is 0.15 mol L^{-1}.

3.2. Structural analysis on powders

Fig. 2 shows the phase evolution of $La_2NiO_{4+\delta}$ powders characterized by XRD analyses. A diffuse XRD patterns is obtained for the powder heat treated at 650°C, indicating that the precursor is amorphous (not reported in this figure). For temperatures above 700°C the La_2NiO_4 phase forms, as shown by the XRD patterns. No reaction is observed by XRD analyses for temperatures up to 800°C. Thus, $La_2NiO_{4+\delta}$ is likely to nucleate from an inorganic amorphous matrix. No intermediate phase is observed. However, the weight loss at 700°C corresponds to the formation of an intermediate phase according to Gaudon's works on LSM [10]. In this work, we do not detect this mixed oxyhydroxycarbonate by XRD and this could be associated with the low level of crystallinity of the phase.

In addition, the annealing time 2–6 h at 900°C or 1000°C does not change the symmetry of the structure, which indicates the formation of a relatively stable phase.

The X-ray diffraction pattern of $La_2NiO_{4+\delta}$ calcinated at 1000°C in air for 2 h is studied by the Rietveld method. The Rietveld refinement profile is shown in Fig. 3. From this result, one observes an orthorhombic unit of La_2NiO_4 (*Fmmm* space group) with $a = 5.458$ (6) Å and $b = 5.463$ (2) Å, $c = 12.686$ (1) Å.

This result is confirmed by the construction of the reciprocal lattice from different electron diffraction patterns [11].

This symmetry in the literature has been found for non-stoichiometry level above 0.13 at room temperature [12,13]. Moreover, Skinner [12] has studied $La_2NiO_{4+\delta}$ oxides having δ of 0.18, using in situ high temperature neutron diffraction. He found that the structure of this sample at room temperature is *Fmmm* orthorhombic with lattice parameters of: $a = 5.45864$ (9) Å and $b = 5.46360$ (4) Å, $c = 12.68524$ (4) Å [12].

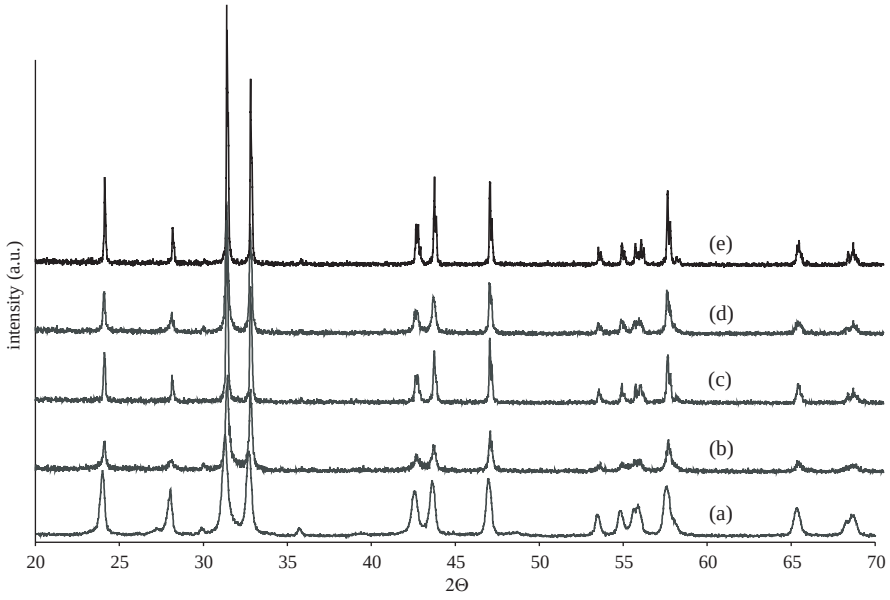

Fig. 2. X-ray diffraction of $La_2NiO_{4+\delta}$ powders calcinated in air at various temperatures. (a) 800°C—2 h, (b) 900°C—2 h, (c) 900°C—6 h, (d) 1000°C—2 h, (e) 1000°C—6 h.

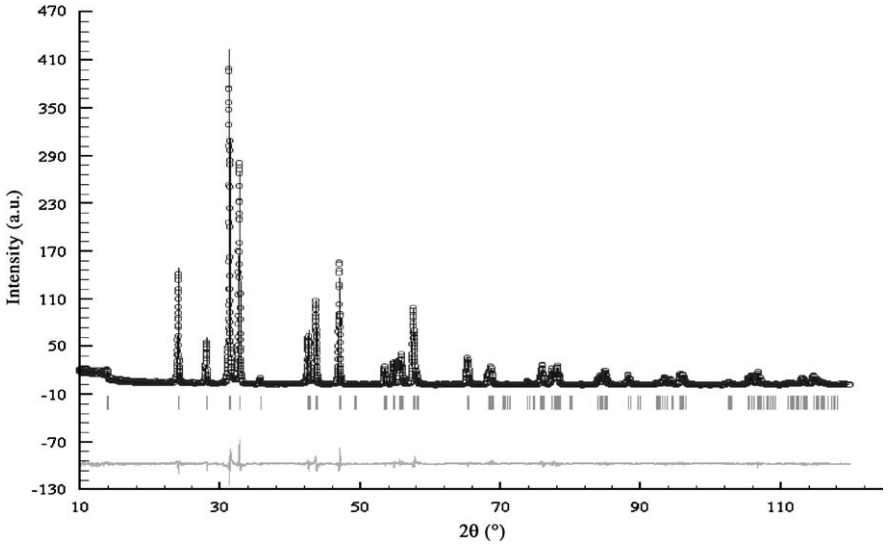

Fig. 3. Rietveld refinement profile for orthorhombic (*Fmmm*) $La_2NiO_{4+\delta}$ at 25°C.

In order to confirm that orthorhombic symmetry is obtained when the non-stoichiometry level in $La_2NiO_{4+\delta}$ is high, δ has been evaluated by both TG analyses under reductive atmosphere (TPR) [11] and chemical titrations [6]. Values are reported in Table 1. For comparison, Table 1 also shows the average of grains size evaluated from Scanning Electron Microscopy and the lattice parameters determined by X-ray analyses.

The non-stoichiometry values evaluated from TPR and chemical titrations are similar. Previously, it has been established that this non-stoichiometry is due to an excess of oxygen and to compensate charge of Ni^{3+} ions formed (hole). These stabilize the K_2NiF_4 structure by both reducing the intrinsic charge separation between the electropositive La_2O_2 and NiO_2 layers and the structural strain due to the misfit between these two layers [14]. These cationic oxidations allow preserving the overall electrical neutrality of the crystals.

The non-stoichiometry level is a function of the partial oxygen pressure and the heating temperature. In these synthesis conditions, the samples are heated in air and the oxygen partial pressure depends on the organic compounds. Indeed, the nature and the content of the organics modify the atmosphere during the decomposition of the dried-gel and thus, have a strong impact on the structure and the stabilization of the excess oxygen content of the resulting oxide [5].

Table 1
Evolution of δ as a function of the lattice parameters with HMTA resins for $R=2$ and 3

Synthesis parameters R, T	δ TGA (± 0.01)	δ chemical titrations (± 0.01)	$\langle d \rangle$ (± 10 nm)	Lattice parameters	Lattice volume
$T=900$°C 2 h $R=2$	0.18	0.19	120 nm	$a=5.4585$ Å $b=5.4629$ Å $c=12.6978$ Å	379 Å^3
$T=1000$°C 2 h $R=2$	0.18	0.18	160 nm	$a=5.4586$ Å $b=5.4632$ Å $c=12.6861$ Å	378 Å^3
$T=900$°C 2 h $R=3$	0.23	0.23	225 nm	$a=5.4578$ Å $b=5.4653$ Å $c=12.6985$ Å	379 Å^3
$T=1000$°C 2 h $R=3$	0.22	0.23	250 nm	$a=5.4578$ Å $b=5.4659$ Å $c=12.6930$ Å	378 Å^3

Table 2
Comparison of δ for oxides prepared with different organics agents and contents (R) and calcined at 900°C and 1000°C in air

Synthesis process	Synthesis parameter (R,T)	δ chemical titration (± 0.01)	$\langle d \rangle$ (nm) (± 10 nm)
HMTA resins	$R=2$, $T=1000$	0.18	160
	$R=3$, $T=1000$	0.22	250
	$R=2$, $T=900$	0.19	120
	$R=3$, $T=900$	0.23	225
Citric acid/ethylene glycol resins	$R=2$, $T=1000$	0.16	100
	$R=3$, $T=1000$	0.16	110
	$R=2$, $T=900$	0.17	80
	$R=3$, $T=900$	0.17	90

The heating of powders at high temperature gives rise to oxides with the lowest excess of oxygen. A correlation between δ and lattice parameters is found. This result is in agreement with the one found in the literature [12,15]. It can be observed a slight decrease of the a parameter from 5.4586 to 5.4578 Å and an increase of the c parameter from 12.6861 to 12.69 Å with increasing δ. Jang et al. [15] have correlated it to the excess of oxygen incorporated into the crystals. They found that the linear increase of the c parameter with δ is mainly due to the expansion of the La–La distance along the c-axis when the variation of δ is small and by an increase of the sum of the La–O and Ni–O distances along the c-axis when the variation of δ is high. On the other hand, the Ni–O distance along the a-axis is slightly reduced for high δ values. Studies performed by Skinner [12] conduced to the same behavior for the La–O and Ni–O distances along the c-axis when increasing the excess oxygen. Indeed, the structure adopts the presence of excess oxygen by modifying the length of these bonds, hence maintaining the lattice volume as shown in Table 1.

3.3. Non-stoichiometry and microstructure of powders

In this table is also reported the value of $\langle d \rangle$ mean diameter evaluated from SEM measurements. In addition, from Rietveld refinement results, the average size of the crystallites is calculated and from the MET micrographs, the average size of the grains size is evaluated. The average size is 110–150 nm for crystallites and 130–160 nm for the grains. Theses values are similar to the one found from SEM experiments. It can be observed an increase of the mean grains size with the heating temperature and the R ratio. Furthermore, in our processes, a correlation between the non-stoichiometry level and the mean grain size appears: the average of grains size increases while δ increases and this evolution seems to be quite linear for the samples studied. An increase of $\langle d \rangle$ from approximately 50 nm is attended with an increase of δ from about 0.015 when powders are heated under air.

To confirm this evolution, other sets of experiments have been carried out by changing the nature of chelating and polymeric agents in order to prepare materials with different non-stoichiometry levels and grain sizes. The chelating agent was citric acid while the polymeric one is ethylene glycol.

The non-stoichiometry ratio of this new route referenced as P2 was determined from similar experiments: TPR and Chemical titrations (Table 2 and Fig. 4). Some of the characterization results are also given in Table 2. As illustrated in this table, δ depends

on the heating temperature and differs from both processes. In our range of temperature, the higher values of δ are obtained for oxides prepared from HMTA process with the higher content of organics compounds. This result confirms the influence of the nature and the content of organics on the non-stoichiometry level and are explained by the variation of the partial oxygen pressure during the decomposition of the sol.

Moreover, as previously shown for HMTA process, δ is also related to the grains size of the oxide prepared from P2 process. The higher the heating temperature, the higher the mean particles size, the lower the non-stoichiometry level.

Indeed, increasing the annealing temperature conduces to an increase of the particles size meanwhile the reduction of the nickel ions from 3+ to 2+ appears.

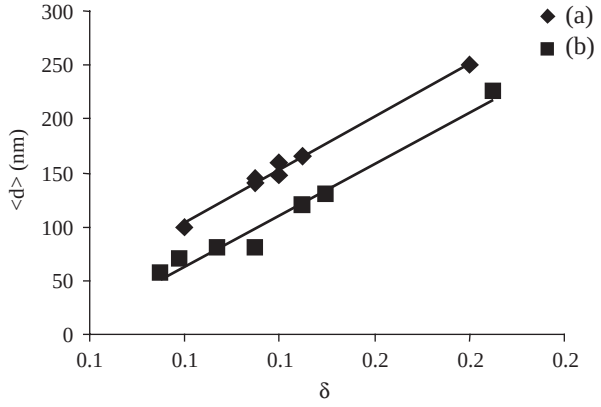

Fig. 4. Evolution of $\langle d \rangle$ as a function of the heating temperature and the non-stoichiometry level in $La_2NiO_{4+\delta}$ powders calcined in air. (a) $T=1000°C$; (b) $T=900°C$.

This reduction is not affect by the initial level of Ni^{3+} issued from the decomposition of the sol, and its evolution is similar whatever the initial level of Ni^{3+} (τ) considered. Thus, if we consider two samples with a difference in τ of 0.04 at 600°C, the increase of the heating temperature at 1000°C for both samples will conduce to the same difference in τ of 0.04. Then, as the synthesis conditions are more oxidizing and the sol decomposition faster for HMTA process (Fontaine, in progress), the level of Ni^{3+} and the particles sizes are higher than the one obtained for samples elaborated by the P2 process for the same conditions.

A comparison of this set of data with the one obtained in the HMTA process shows the impact of the chemical route on δ. Indeed, one can see clearly that δ reaches a value of 0.18 for $T=1000°C$ in the HMTA process while for the same temperature, δ is about 0.16 in the P2 process.

3.4. Structural analysis of thin films

Grazing angle X-ray diffraction patterns of the $La_2NiO_{4+\delta}$ thin films synthesized are obtained for films synthesized with a viscosity of 40 cP and calcinated at 900°C and 1000°C in air during 2 h. Fig. 5 shows the results obtained for thin films (85 and 90 nm, respectively) using a grazing angle of 1°. Under these conditions, the peaks corresponding to the YSZ substrate can be observed, which indicate that the X-ray beam goes through the $La_2NiO_{4+\delta}$ film. Only $La_2NiO_{4+\delta}$ phase peaks with the K_2NiF_4 structure are observed. However, it is difficult to determine the phase symmetry of the film due the limit of resolution of the apparatus.

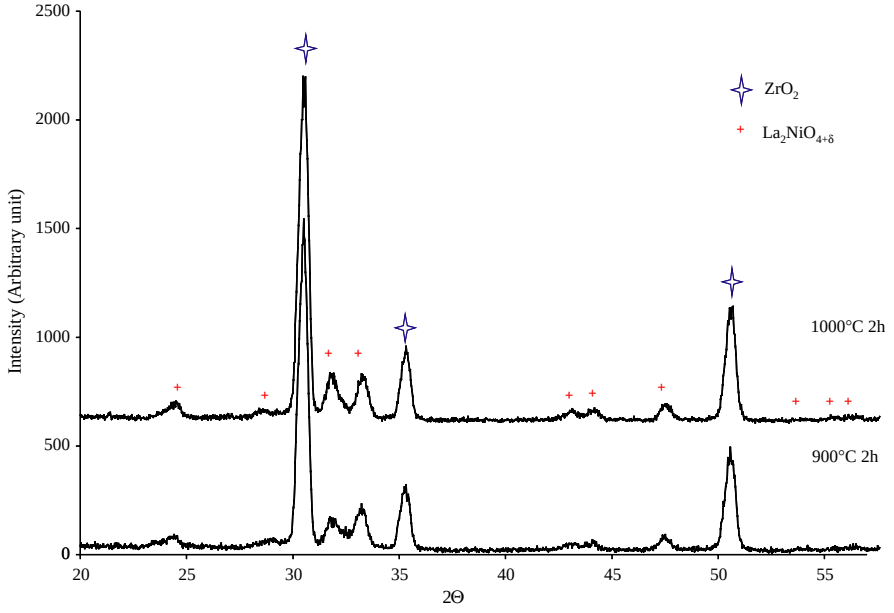

Fig. 5. Grazing angle X-ray diffraction patterns of film deposited on YSZ substrate and annealed at 900°C and 1000°C in air for 2 h.

A comparison of the X-ray diffraction patterns obtained on powders and thin films shows that the position of the peaks is the same. This implies that the symmetry of the film is orthorhombic and that there is no constraint in the film. In addition, a study of peaks intensity of XRD films shows that our films are polycrystalline with a random orientation. According to results obtained on powders, the orthorhombic symmetry is obtained for high non-stoichiometry levels [16].

3.5. Non-stoichiometry and microstructure of films

The effects of the viscosity and the heating temperature on the microstructure of thin films are then studied. Fig. 6 reports Scanning Electron Microscopy micrographs of $La_2NiO_{4+\delta}$ thin films deposited onto YSZ substrates for different heating temperatures and viscosities. The microstructure of the film depends on the processing parameters. As it can be observed, whatever the conditions used, one obtains a crack-free film with a smooth surface. The roughness of the film is small and lower than 10 nm [11]. For a heating temperature of 800°C, the viscosity of the polymeric sols influences the surface morphology of the film. When the viscosity is low, films have no defined grain size, indicating the poor crystallinity of the film. However, an increase in viscosity allows synthesizing a denser film. This result can be correlated to the concentration of water in the polymeric sol because the ratio of organic compounds to transition metal oxides is always the same. Indeed, the higher the viscosity, the lower the water concentration in the sol, and thus the denser the microstructure.

Another parameter is directly related to the films density: the heating temperature. Figs. 6a and d show the SEM of the $La_2NiO_{4+\delta}$ thin films annealed at 800°C and 1000°C for 2 h. A crack-free film with a smooth surface and with a well-defined grain structure is obtained for $T = 1000$°C. This well-defined grain structure for the films indicates that it has a fine microstructure. Grains constituted of nanometric crystallites formed it. While increasing the heat treatment, these clusters or domains of small crystallites sinter to form a dense and crack-free granular microstructure. This type of microstructure leads to the formation of smooth surfaces as shown in Fig. 6c micrograph. Compared to Fig. 6a, one observes a rearrangement of crystalline domains.

According to thermal analysis results as well as XRD and SEM results, the following microstructural evolution step by step of the $La_2NiO_{4+\delta}$ thin films, prepared from polymeric precursors, can be proposed: (a) formation of clusters of nanometric crystals from an amorphous matrix; (b) densification of clusters resulting in a microstructure consisting of small grains domains, (c) densification or grain growth of the small grain domains forming a polycrystalline microstructure with granular texture, low porosity and a smooth surface.

The grain size exhibits important modifications with heat treatment temperatures. At 800°C, one observes a fine grain structure with grains on the order of 20 nm. An increase in the heat treatment temperature further to

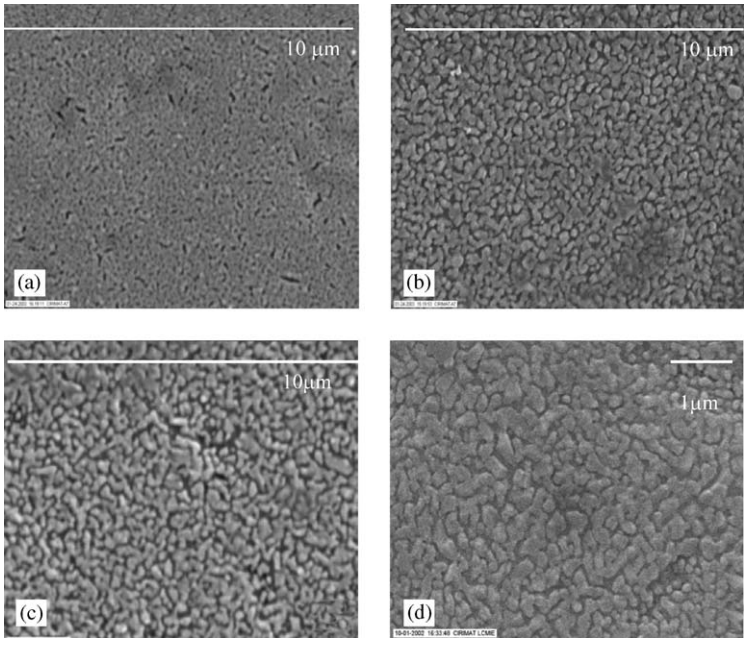

Fig. 6. SEM micrographs of $La_2NiO_{4+\delta}$ thin films deposited on YSZ substrate annealed for 2 h: (a) $T = 800$°C, $\eta = 40$ cP; (b) $T = 1000$°C, $\eta = 40$ cP; (c) $T = 1000$°C, $\eta = 30$ cP; (d) $T = 1000$°C, $\eta = 51$ cP.

1000°C results in an increase of the grain size to approximately 140 nm.

It was difficult to determine the non-stoichiometry level of the film oxides from the results obtained for powders synthesized in the same conditions. Indeed, we should consider that the oxygen partial pressure applied during the transition 'polymeric film-oxide film' is different from the one applied during the decomposition of the powders as the content of organics differs. Moreover, the surface exchange of both films and powders is also different. However, from our results, we can predict that the increase of the heat temperature from 900°C to 1000°C should conduce to a slight decrease of δ as shown for powders. As the non-stoichiometry level is strongly correlated to the content of organics, we can also assume that the thickness of the polymeric film deposited before the heat treatment strongly influences the non-stoichiometry of the film oxide. Then, thicker films should generate more oxidizing atmosphere during their decomposition in air. In our samples, we presume that their δ is relatively similar as there is no significant change in their thickness (Table 3).

The synthesis process allows a control of the non-stoichiometry level by modifying the heating temperature. In addition, the non-stoichiometry level can be adjusted by modifying the nature of the chelating and polymeric agents used during the synthesis of the dip-coated solution [11]. Thus, a large variety of non-stoichiometry for thin films could be obtained.

This control is interesting for the preparation of cathode materials for SOFC applications. Indeed, both the electrical conductivity and the ionic conductivity depend on the non-stoichiometric level: good electrical conductivity is obtained for materials exhibiting high non-stoichiometric coefficients although good ionic conductivity for materials having low non-stoichiometry level. Thus, a compromise in terms of non-stoichiometry should be found in order to reach both a good electrical and a good ionic conductivity.

The thickness of the $La_2NiO_{4+\delta}$ thin films evaluated by rugosimetry measurements has been studied. The evolutions of the film thickness as a function of the sol viscosity for different heat treatments (temperature and time at the dwelling temperature) are reported in Fig. 7. The film thickness increases with the viscosity whatever the heating temperature. This evolution follows the Landau Levich law [17]. The higher the thickness, the higher the viscosity.

The influence of the dwelling time at various temperatures on the thickness has been also studied. As it can be seen, the dwelling time has no influence on the film thickness. The highest thickness is about 80 nm and is achieved for a viscosity of 60 cP. These studies show that there is no influence of the time and the heating temperature on the thickness of thin films. The highest thickness reached for one coating is too small for the application of these materials in SOFC devices. But making thicker films is possible increasing the number of coatings during the synthesis of the film. In addition,

Table 3
Evolution of the viscosity of the sol and the mean grain size $<d>$ of the film as a function of the heat treatment. The R ratio of the sol is remained at 2.

Synthesis parameters (R,T)	Viscosity (cP)	$\langle d \rangle$ (nm) (± 10 nm)
$T=900$°C—6 h: 00	22	57
$R=2$	30	70
	38	80
$T=1000$°C—6 h: 00	30	140
$R=2$	40	145
	51	148

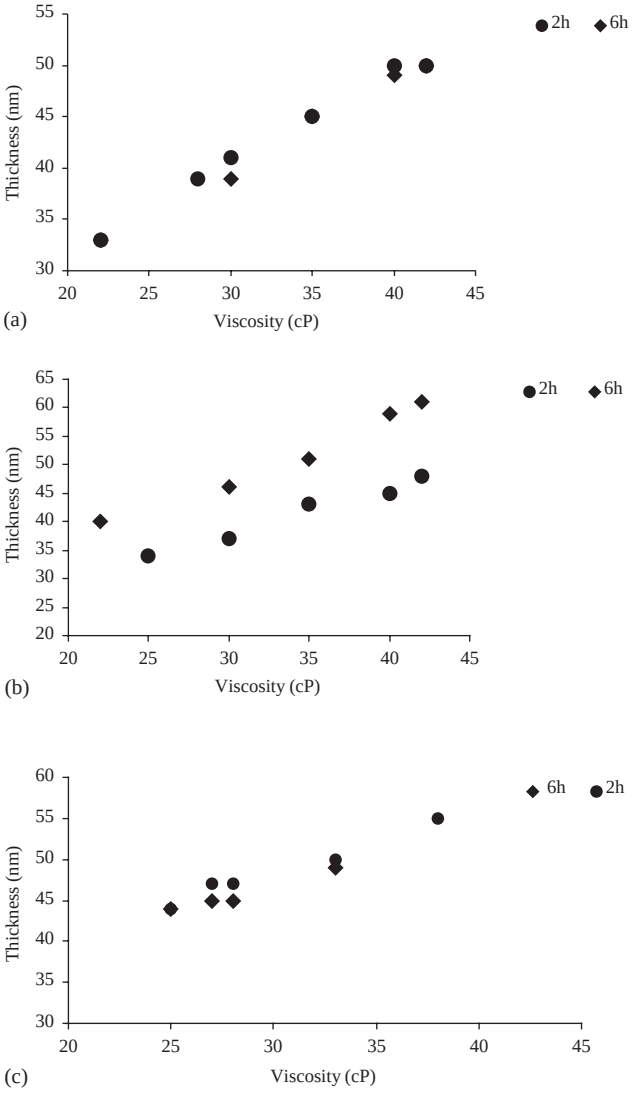

Fig. 7. Thickness evolution as a function of the viscosity for different temperatures and a withdrawal speed of 1.7 cm min^{-1}: (a) $T=1000$°C; (b) $T=900$°C; (c) $T=800$°C.

these results show that despite the small thickness of the layer, it is possible to elaborate films with different porosities by controlling the viscosity of the polymeric sols. The control of the microstructure is critical for a good system performance of SOFC devices. Indeed, the reduction of the oxygen depends both on the cathode composition and on the microstructure [16,18]. When the cathode material is a mixed conductor, the microstructure has to be dense in order to minimize ohmic losses. Thus, the elaboration of dense $La_2NiO_{4+\delta}$ materials via a polymeric method is important for SOFCs.

4. Conclusion

Homogeneous, crack-free, dense thin $La_2NiO_{4+\delta}$ films with Ruddlesden Popper structure have been prepared onto YSZ substrates using a polymeric precursor synthesized via a chemically modified Pechini process. The XRD results show that the film is polycrystalline with a random orientation. Extrapolations between the average grains size and the non-stoichiometry level on powders have been made in our processes. Moreover, an estimation of the film non-stoichiometry evolution as a function of the thickness of the polymeric film has been discussed in this paper considering that the nature and the content of organics control the non-stoichiometry level of the film.

Correlations between the sol viscosity, the calcination temperature and the microstructure of the film are determined. Indeed, the thickness of the films evolves with the viscosity. An increase in the viscosity leads to an increase of the thickness of the films up to 80 nm. However, the heating temperature does not affect the thickness of the film for films heat-treated at 800°C and 1000°C. The heat treatment only modifies the microstructure. A denser structure is obtained for a higher temperature, 1000°C. Thus, using a polymeric method, the microstructure of the films can be adjusted by controlling the processing parameters.

Acknowledgments

The authors thank Dr. A. Barnabé for his help for the Rietveld study.

References

[1] P. Stevens, F. Novel-Cattin, A. Hammou, C. Lamy, M. Cassir, Les piles à combustible, Tech. Ing. D5 (2000) 3340.
[2] E. Ivers-Tiffee, A. Weber, D. Herbstritt, J. Eur. Ceram. Soc. 21, (2001) 10–11, 1805–1811.
[3] K. Sasaki, J.P. Wurthe, M. Godickemeier, A. Mitterdorfer, L.J. Gauckler, M. Dokiya, O. Yamamoto, H. Tagawa, S.C. Singhal (Eds.), Proceeding of the Fourth International Symposium on SOFC, Yokohama, Japan, 1995, p. 625.
[4] M. Gaudon, C. Laberty-Robert, F. Ansart, P. Stevens, A. Rousset, Solid State Sciences 4 (2002) 125–133.
[5] V.V. Vashook, I.I. Yushkevich, L.V. Kokhanovsky, L.V. Makhnach, S.P. Tolochko, I.F. Kononyuk, H. Ullmann, H. Altenburg, Solid State Ionics 119 (1999) 23–30.
[6] E. Boehm, J.M. Bassat, M.C. Steil, P. Dordor, F. Mauvy, J.C. Grenier, Solid State Ionics 5 (2003) 973–981.
[7] V.V. Kharton, A.P. Viskup, A.V. Kovalesky, E.N. Naumovich, F.M.B. Marques, Solid State Ionics 143 (2001) 337–353.
[8] V.V. Vashook, S.P. Tolochko, I.I. Yushkevich, L.V. Makhnach, I.F. Kononyuk, H. Altenburg, J. Hauck, H. Ullmann, Solid State Ionics 110 (1998) 245–253.
[9] Pechini, Patent, 3.330.697, July 11 (1967).
[10] M. Gaudon, C. Laberty-Robert, F. Ansart, P. Stevens, A. Rousset, Solid State Sci. 4 (2002) 125–133.
[11] M.L. Fontaine, C. Laberty-Robert, F. Ansart, P. Tailhades, Fuel Cell Conference, Forbach, Proceeding FDFC2002n. 044. October 2002, pp. 240–247.
[12] S. Skinner, Solid State Sci., in press.
[13] J.M. Tranquada, Y. Kong, J.E. Lorenzo, D.J. Buttrey, D.E. Rice, V. Sorcham, Phys. Rev. B 50 (1994) 6340.
[14] M. Greenblatt, Solid State Mater. Sci. 2 (1997) 174–183.
[15] W.J. Jang, K. Imai, M. Hasegawa, H. Takei, J. Crystal Growth 152 (1995) 158–168.
[16] D.E. Rice, D.J. Buttrey, J. Solid State Chem. 105 (1–2) (1993), 181–188.
[17] C.J. Brinker, G.W. Scherer, Sol Gel Sci. (1990) 788–795.
[18] H. Kamata, A. Hosuka, J. Mizusaki, H. Tagawa, Solid State Ionics 106 (1998) 237.